ISBN: 978-3-95450-179-3 doi:10.18429/JACoW-FEL2017-MOP021

SIDEBAND SUPPRESSION IN TAPERED FREE ELECTRON LASERS*

Cheng-Ying Tsai[1†], Juhao Wu[1‡], Chuan Yang[1,2], Moohyun Yoon[1,3], and Guanqun Zhou[1,4]
[1]SLAC National Accelerator Laboratory, Menlo Park, California, USA
[2]NSRL, University of Science and Technology of China, Hefei, Anhui, China
[3]Department of Physics, Pohang University of Science and Technology, Pohang, Korea
[4]Institute of High Energy Physics, and UCAS, Chinese Academy of Sciences, Beijing, China

Abstract

It is known that in a high-gain tapered free electron laser (FEL) there is the so-called second saturation point where the FEL power ceases to grow. Sideband instability is one of the major reasons causing this second saturation. Electron synchrotron oscillation coupling to the sideband SASE radiation leads to the appearance of sidebands in the FEL spectrum, and is believed to prevent a self-seeding tapered FEL from reaching very high peak power or improved spectral purity without resorting to external monochromators. In this paper, we propose a simple method of using phase shifters to suppress the undesired sideband signal. This method requires no external optical device and so is applicable at any wavelength. The phase-shift method is implemented in the post-saturation regime where the main signal shall have reached its available power level. Numerical simulations based on Pohang Accelerator Laboratory x-ray FEL beam and undulator system confirm the effectiveness of this method. The results show that the sideband signals are clearly suppressed while the main signal remains a comparable level to that without employing such a method.

INTRODUCTION

Generating an intense high-power x-ray free electron laser (FEL) can be of great interest, e.g. the pulse power at the level of ~50 GW, since such power level of output radiation has stimulated numerous experiments in various scientific areas [1–3]. The output characteristics of FEL are determined by its operation modes (see, for example, Ref. [4] for introduction of short-wavelength FEL basics). In the x-ray wavelength regime a single-pass high-gain FEL can work either in the Self-Amplified Spontaneous Emission (SASE) or seeded mode, despite the lack of direct seeding source. In the SASE mode [5], the initial seeding originates from shot noise of the electron beam. Therefore the output characteristics of SASE can be chaotic in both temporal and spectral profile, although the transverse coherence can be excellent. Acting as an amplifier, the seeded mode indeed requires an input source. It has been known that utilizing higher harmonics generation, e.g. high-gain harmonics generation (HGHG) [6, 7] or echo-enabled harmonic generation (EEHG) [8, 9], can be an option. Another option is the so-called self-seeding [10–12]. In the self-seeding option the FEL system starts with the first section of undulators based on SASE mode and is followed by a crystal monochromator or mirrors to select/purify the output spectrum, serving as the subsequent input signal. Then a second section of undulators proceeds, acting as an amplifier, and will amplify the (purified) signal, i.e. the main signal, up to saturation. Compared with SASE, the output characteristics of seeded FEL are in general with much narrower spectral bandwidth and better wavelength stability.

In some applications when an even higher pulse power can be desired, e.g. the femtosecond x-ray protein nanocrystallography, single molecule imaging and so on, dedicated undulator taperings are typically employed [13–16]. Recently the efficiency enhancement based on phase jump method is also proposed [17]. In other situations when the temporal coherence or spectral brightness may be benefited or even required, e.g. the resonant scattering experiment, mixing-wave experiment or those which rely on spectroscopic techniques, the seeded mode shall be considered. However, the higher spectral purity may be prevented by the so-called FEL sideband instability (see, for example, [13, 18–20]). Such instability in FEL is caused by the interaction of the radiation field with the electron synchrotron motion in the ponderomotive potential well after the first saturation of FEL. Such a potential well, formed by the undulator magnetic field and the main signal, will trap electrons and result in the oscillation with a synchrotron frequency (and its multiples) away from the resonance frequency (i.e. the frequency of the main signal). Once the interaction creates a positive feedback, the electron beam energy will continuously transfer and contribute to the electromagnetic field with the specific synchrotron sideband frequency. Then the sideband signal will grow and the output radiation spectrum will feature a main-signal peak with surrounding sideband peaks or a pedestal-like structure. This usually brings about undesirable consequences; the sideband effect can not only degrade the spectral purity but also limit the level of the saturation power of FEL. Employing a post-undulator monochromator may help clean the sideband structure. A dedicated monochromator however depends on specific wavelength range or photon energy and may limit the tunability. The method introduced here requires no external optical device and so is applicable at any wavelength.

In this paper we propose a simple method of using a set of phase shifters to suppress the undesired sideband signal. As mentioned above, because the phase shifters used for

* The work was supported by the US Department of Energy (DOE) under contract DE-AC02-76SF00515 and the US DOE Office of Science Early Career Research Program grant FWP-2013-SLAC-100164.
† jcytsai@SLAC.Stanford.EDU
‡ jhwu@SLAC.Stanford.EDU

ISBN: 978-3-95450-179-3 doi:10.18429/JACoW-FEL2017-MOP021

sideband suppression will not likely enhance the main signal, they should be placed where the main signal has reached its desired power level in a prescribed undulator tapering, i.e. those phase shifters with sideband-suppression purpose should not be placed too early. It should be also noted that the phase shifters should not be placed too late, where the sideband signal would have been dominant.

THEORETICAL ANALYSIS

The study is based on 1-D FEL analysis [4], where the individual particles in an electron beam are characterized by the electron relative phase $\theta = (k_u + k_1)z - \omega_1 t$ and energy deviation $\eta = (\gamma - \gamma_R(0))/\rho\gamma_R(0)$ from a reference particle with the energy γ_R. Here t and z are the time and undulator coordinates. k_u and k_1 are the wavenumbers of the undulator and the resonant signal (or the main signal), respectively. $\lambda_{1,u} = 2\pi/k_{1,u}$, $\omega_1 = ck_1$. ρ is the usual FEL or Pierce parameter. The FEL resonance condition is $\lambda_1 = \lambda_u\left[1 + K^2(z)/2\right]/2\gamma_R^2(z)$. In a tapered FEL, $K(z) = K_0 f_B(z)$ with the taper profile $0 \leqslant f_B(z) \leqslant 1$. Correspondingly we have $\gamma_R(z) = \gamma_R(0) f_R(z)$ with $f_R(z) = \sqrt{\left(1 + K^2(z)/2\right)/\left(1 + K_0^2/2\right)}$. In the 1-D analysis the electrons are described by the following equations [13,18,20,21]

$$\frac{d\theta}{d\hat{z}} = \frac{\eta - \eta_R}{f_R} \tag{1}$$

$$\frac{d\eta}{d\hat{z}} = -\frac{f_B}{f_R}\left(\mathcal{E}e^{i\theta} + \text{c.c.}\right) \tag{2}$$

where $\hat{z} = 2k_u\rho z$, $\mathcal{E}$ is the normalized complex electric field, $\mathcal{E} = E\Big/\sqrt{4\pi n_0\rho\gamma_{R0}m_0c^2}$, and c.c. denotes the complex conjugate. In the aftermath of the appreciable main signal growth, it can be shown that the main signal behaves as a low-gain FEL[1]. In the post-saturation regime the low-gain enhancement by virtue of energy detuning may be limited because the phase space should have been populated by electron beam particles with appreciable energy spread, i.e. the warm beam.

Note that although the (large) main signal can follow low-gain FEL process, the (small) sideband signal after saturation can grow exponentially. The field dynamics is governed by the slowly-varying wave equation, $d\mathcal{E}/d\hat{z} = (f_B/f_R)\left\langle e^{-i\theta}\right\rangle$. For simplicity we only consider two-frequency model, i.e. $\mathcal{E} = \mathcal{E}_1 + \mathcal{E}_s = |\mathcal{E}_1|\, e^{i\phi_1} + \left|\mathcal{E}_s^{\pm}\right| e^{i\nu_{\pm}\phi_1}$ with $\left|\mathcal{E}_s^{\pm}\right| \ll |\mathcal{E}_1|$. In what follows, the subscripts 1 and s here refer to the main and the sideband signal, respectively. Here ϕ_1 is the phase of the main signal and $\nu_{\pm} = 1 \pm \Delta\nu = \omega/\omega_1$ with the frequency detuning of upper sideband signal ($\Delta\nu > 0$) and the lower sideband signal ($\Delta\nu < 0$). Our analysis begins with separating the complex electric field into the main signal and the sideband signals

$$\frac{d\mathcal{E}_1}{d\hat{z}} = \frac{f_B}{f_R}\left\langle e^{-i\theta}\right\rangle \tag{3}$$

$$\left(\frac{d}{d\hat{z}} + i\frac{\Delta\nu}{2\rho}\right)\mathcal{E}_s = \frac{f_B}{f_R}\left\langle e^{-i\nu\theta}\right\rangle \tag{4}$$

We then further rewrite the main and sideband field equations into their amplitude and phase components, which lead to the following four equations

$$\frac{d\,|\mathcal{E}_1|}{d\hat{z}} = \frac{f_B}{f_R}\cos\Theta \tag{5}$$

$$|\mathcal{E}_1|\,\frac{d\phi_1}{d\hat{z}} = -\frac{f_B}{f_R}\sin\Theta \tag{6}$$

$$\left(\frac{\partial}{d\hat{z}} + i\frac{\Delta\nu}{2\rho}\right)\left|\mathcal{E}_s^{\pm}\right| = \frac{f_B}{f_R}\cos\nu_{\pm}\Theta \tag{7}$$

$$\left|\mathcal{E}_s^{\pm}\right|\frac{d\phi_s^{\pm}}{d\hat{z}} \pm \frac{|\Delta\nu|}{2\rho}\left|\mathcal{E}_s^{\pm}\right| = -\frac{f_B}{f_R}\sin\nu_{\pm}\Theta \tag{8}$$

where $\Theta = \theta + \phi_1$ denotes the ponderomotive phase.

In adjusting a phase shifter between two consecutive undulator segments, the relative electron phase $\Delta\theta$ is changed. Assuming the radiation pulse travels along a phase shifter with negligibly small phase change ($\Delta\phi_1 \approx \tan^{-1}(L^{PS}/z_R) \approx \tan^{-1}(1/15) \approx 4°$ where L^{PS} is the section length of a phase shifter, assumed 1 m, and z_R is the Rayleigh length, typically in the range of 10 ~ 20 m), the ponderomotive phase change can be approximately quantified as $\Delta\Theta \approx \Delta\theta$. The goal is to arrange the electron beam within the phase of decelerating the sideband signal ($\cos\nu_{\pm}\Theta < 0$), while the main signal should remain constant ($\cos\Theta \approx 0$). Prior to a phase shifter, we assume the averaged ponderomotive phase over the electron bunch coordinate θ and beamlet slices s does not change too much, i.e. $\langle\Theta\rangle_{\theta,s} \approx 0$, during the passage in the undulator. Our numerical simulations support this assumption. A phase shifter is assumed to delay all particles of the electron beam relative to the radiation. After the phase shifter, the rate of change of the main signal is proportional to $\cos\Delta\theta$ [see Eq. (5)], while that of the sideband becomes $\cos\Delta\theta \mp |\Delta\nu|\,\Delta\theta\sin\Delta\theta$ [see also Eq. (7)]. Note that the detuning parameter $|\Delta\nu| \sim 10^{-3} \ll 1$. It can be easily found that $\Delta\theta \approx \pi$ (or its odd integer multiples) can meet the requirement.

NUMERICAL RESULTS

We take as an example the Pohang Accelerator Laboratory x-ray FEL (PAL-XFEL) beam and undulator system [23]. Table 1 summarizes the relevant beam, undulator and radiation parameters. The FEL operation mode is assumed to start from SASE in the first undulator section and then self-seeding in the second undulator section. It is assumed that in the second undulator section the system consists of 22 planar undulators, with 4.94 m for each undulator segment

[1] We can Taylor expand the electron energy and phase coordinates as $\eta = \eta^{(0)} + \eta_1^{(1)} + \eta_1^{(2)} + \eta_s^{(1)} + \ldots$ and $\theta = \theta^{(0)} + \theta_1^{(1)} + \theta_s^{(1)} + \ldots$, respectively. To be clear, the subscripts 1 and s here refer to the main and the sideband signal, respectively. It can be shown that Madey's first theorem [22] $\left\langle\eta_1^{(2)}\right\rangle = (1/2)\,\partial\left\langle\left(\eta_1^{(1)}\right)^2\right\rangle\Big/\partial\eta^{(0)}$ can be obtained (where the bracket $\langle\ldots\rangle$ denotes the phase average of the electron beam macroparticles), and the low-gain function can be formulated as $G \propto -\hat{L}_u^2\,\partial\left[\sin\left(\eta^{(0)}\hat{L}_u\right)\Big/\eta^{(0)}\hat{L}_u\right]^2\Big/\partial\eta^{(0)}$ (where $\hat{L}_u = 2k_u\rho L_u$ is the normalized undulator segment length) in the absence of undulator tapering [4].

ISBN: 978-3-95450-179-3 doi:10.18429/JACoW-FEL2017-MOP021

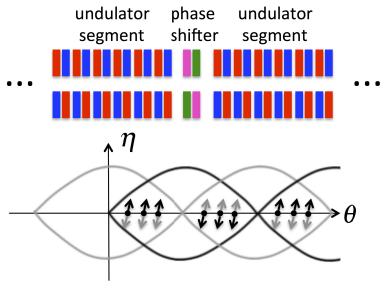

Figure 1: Two consecutive undulator segments with a phase shifter (a small by-pass chicane) in between to delay the relative electron phase to the radiation. The number and strength of the phase shifter is determined by optimizing the ratio of the main to the sideband signals. The longitudinal phase space plot above is to illustrate the purpose of our phase shift method to suppress sideband. The gray and black colors refer to the situations before and after the phase shift. The phase delay will cut out the electron synchrotron motion and therefore suppress sideband signal. The FEL field energy remains constant because the electrons first give and then absorb the energy before and after the phase change.

Table 1: The Relevant Beam, Undulator, and Radiation Parameters for PAL Hard X-Ray FEL

Name	Value	Unit
Electron beam energy	5.885	GeV
RMS fractional energy spread	1.74×10^{-4}	
Peak current	4	kA
Normalized emittances (x, y)	0.4, 0.4	μm
Average beta function (x, y)	10, 10	m
Undulator parameter K_0 (peak)	2.08	
Undulator period	2.6	cm
Input seed power	500	kW
Resonance wavelength	3.1/4	Å/keV
First saturation power	~20	GW
First saturation length	~30	m

and made with variable gaps. The variable undulator gaps enable the undulator tapering up to 15%. Here we only utilize a total ratio of 7% (quadratic) tapering throughout the undulator system. A small by-pass chicane, acting as a phase shifter, is installed between two consecutive undulator segments. In what follows we will present the simulation results in the second undulator section, assuming the seeding power is 500 kW, which is achievable easily in a self-seeded FEL.

We note that the above analysis is based upon 1-D FEL model. In the following we will verify the concept of π phase shift for sideband suppression by using GENESIS [24], a three-dimensional time-dependent FEL simulation code. In GENESIS a phase shifter between two consecutive undulator segments can be modeled using a virtual undulator section. The effective undulator parameter for this section, K_{AD}, should satisfy $\frac{1+K_{AD}^2(z)}{1+K^2(z)} k_u L^{PS} = m\pi$, where m can be an integer or a fraction. A discrete or stepwise undulator tapering is assumed and the optimized tapering profile is based on the algorithm outlined in Ref. [14]. In the above analysis we have assumed the incident ponderomotive phase $\Theta_i = 0$, i.e. assuming most of the electrons are deeply trapped in the bottom of ponderomotive potential well[2]. Figure 2 compares both the integrated power and the main-signal power before and after employment of the π phase shifters. From Fig. 2(a) it can be seen that inserting π phase shifters will result in slight degradation of the integrated power (the black and red solid lines). This can be expected because the π phase shifting, rather than 2π for the constructive interference between FEL radiation and the electron beam, will cut out the effective interaction. The smaller deviation of the red solid and dashed lines indicate that the main-signal power, quantified as $P(\omega) \approx (dP(\omega)/d\omega)\,\delta\omega$, where $dP(\omega)/d\omega$ is the frequency distribution of the total power, appears to be more contributed than the usual case, in which all the phase shifters are simply set to 2π. Figure 2(b) and 2(c) respectively illustrate the resultant FEL radiation spectra for all-2π case and the optimized π-phase-shift case. Here we note that all the π phase shifters should form as pairs, in order that the beam and the radiation can remain in phase in the downstream undulator segments of those π phase shifters.

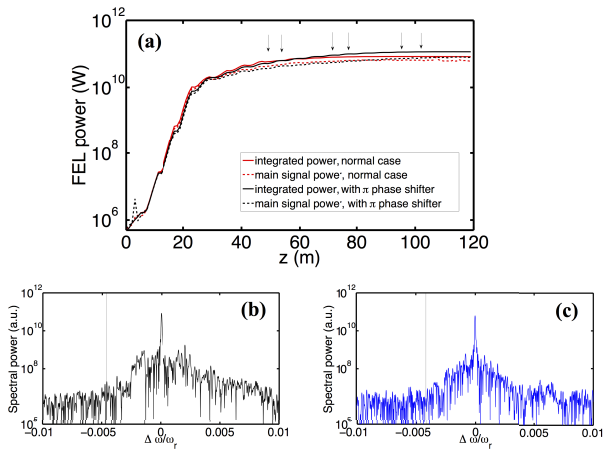

Figure 2: (a) The integrated power and the main signal power as a function of z; (b,c) the radiation spectra for all-2π case and the π-phase-shift case. Here the π phase shifters are inserted at the locations where the arrows in subfigure (a) are indicated.

SUMMARY AND CONCLUSION

From the analysis presented above, we have proposed a simple method of utilizing π phase shifters to effectively suppress the undesired FEL sideband instability. Such a π phase shifter should not be placed in the too-early tapered undulator segments; otherwise it will cut out the (still efficient) interaction between the main signal and the electron beam.

[2] In reality Θ_i may be close to 0 but does not necessarily vanish. To obtain an optimal solution for $\Delta\theta$, we numerically vary $\Delta\theta$ (i.e. K_{AD}) in the nearby value of π (or its odd integer multiples). Note that Fig. 2 presented here is not optimized yet. The numerical optimization is ongoing.

ISBN: 978-3-95450-179-3 doi:10.18429/JACoW-FEL2017-MOP021

Neither should the phase shifters be employed in the too-late undulator segments, where the sideband signal would likely have become dominant. The numerical simulations based on PAL-XFEL beam and undulator parameters have confirmed the analysis. The results show that the pulse power ~50 GW with excellent spectral purity can be achieved by using this simple method.

REFERENCES

[1] H. N. Chapman *et al.*, "Femtosecond X-ray protein nanocrystallography", *Nature* 470 (2011) 73-77. https://doi.org/10.1038/nature09750

[2] M.M. Seibert *et al.*, "Single mimivirus particles intercepted and imaged with an X-ray laser", *Nature* 470 (2011) 78-81. https://doi.org/10.1038/nature09748

[3] A. Fratalocchi and G. Ruocco, "Single-Molecule Imaging with X-Ray Free-Electron Lasers: Dream or Reality?", *Phys. Rev. Lett.* 106 (2011) 105504. https://doi.org/10.1103/PhysRevLett.106.105504

[4] K.-J. Kim, Z. Huang, and R. Lindberg, *Synchrotron radiation and free-electron lasers: Principles of coherent x-ray generation*, Cambridge University Press, 2017.

[5] K.-J. Kim, "Three-Dimensional Analysis of Coherent Amplification and Self-Amplified Spontaneous Emission in Free-Electron Lasers", *Phys. Rev. Lett.* 57, 1871 (1986)

[6] L. H. Yu, "Generation of intense uv radiation by subharmonically seeded single-pass free-electron lasers", *Phys. Rev.* A 44, 5178 (1991).

[7] L.-H. Yu, M. Babzien, I. Ben-Zvi, L. F. DiMauro, A. Doyuran, W. Graves, E. Johnson, S. Krinsky, R. Malone, I. Pogorelsky, J. Skaritka, G. Rakowsky, L. Solomon, X. J. Wang, M. Woodle, V. Yakimenko, S. G. Biedron, J. N. Galayda, E. Gluskin, J. Jagger, V. Sajaev, I. Vasserman, "High-Gain Harmonic-Generation Free-Electron Laser", *Science*, Vol. 289, Issue 5481, pp. 932-934, https://doi.org/10.1126/science.289.5481.932

[8] G. Stupakov, "Using the Beam-Echo Effect for Generation of Short-Wavelength Radiation", *Phys. Rev. Lett.* 102, 074801 (2009).

[9] D. Xiang and G. Stupakov, "Echo-enabled harmonic generation free electron laser", *Phys. Rev. ST Accel. Beams* 12, 030702 (2009).

[10] J. Feldhaus, E. L. Saldin, J. R. Schneider, E. A. Schneidmiller, and M. V. Yurkov, "Possible application of X-ray optical elements for reducing the spectral bandwidth of an X-ray SASE FEL", *Opt. Commun.* 140, 341 (1997).

[11] G. Geloni, V. Kocharyan, and E. Saldin, "A novel self-seeding scheme for hard X-ray FELs", *J. Mod. Opt.* 58 (2011) 1391. https://doi.org/10.1080/09500340.2011.586473

[12] J. Amann *et al.*, "Demonstration of self-seeding in a hard-x-ray free-electron laser", *Nat. Photon.* 6 (2012) 693. https://doi.org/10.1038/nphoton.2012.180

[13] N. Kroll, P. Morton, and M. Rosenbluth, "Free-electron lasers with variable parameter wigglers", *IEEE Journal of Quantum Electronics*, 17(8):1436-1468, August 1981.

[14] Y. Jiao, J. Wu, Y. Cai, A. W. Chao, W. M. Fawley, J. Frisch, Z. Huang, H.-D. Nuhn, C. Pellegrini, and S. Reiche, "Modeling and multidimensional optimization of a tapered free electron laser", *Phys. Rev. ST Accel. Beams*, 15:050704, May 2012.

[15] C. Emma, K. Fang, J. Wu, and C. Pellegrini, "High efficiency, multiterawatt x-ray free electron lasers", *Phys. Rev. Accel. Beams*, 19:020705, Feb 2016.

[16] J. Wu, N. Hu, H. Setiawan, X. Huang, T. O. Raubenheimer, Y. Jiao, G. Yu, A. Mandlekar, S. Spampinati, K. Fang, C. Chu, and J. Qiang, "Multi-dimensional optimization of a terawatt seeded tapered free electron laser with a multi-objective genetic algorithm", *Nuclear Instruments and Methods in Physics Research Section* A: Accelerators, Spectrometers, Detectors and Associated Equipment, 846:56, 2017.

[17] A. Mak, F. Curbis, and S. Werin, "Phase jump method for efficiency enhancement in free-electron lasers", *Phys. Rev. Accel. Beams* 20, 060703 (2017)

[18] S. Isermann and R. Graham, "Suppression of the sideband instability in tapered free-electron lasers", *Physical Review* A, 45:4050, 1992.

[19] S. Riyopoulos, "Sideband suppression in tapered wiggler free electron lasers including thermal spreads", *Physics of Plasmas*, 7(5):1586-1594, 2000.

[20] C.-Y. Tsai, J. Wu, C. Yang, M. Yoon, and G. Zhou, "Analysis of the sideband instability based on an one-dimensional high-gain free electron laser model", submitted to *Phys. Rev. Accel. Beams* (2017)

[21] R. Bonifacio, F. Casagrande, M. Ferrario, P. Pierini, and N. Piovella, "Hamiltonian model and scaling laws for free-electron-laser amplifiers with tapered wiggler", *Optics Communications*, 66(2):133-139, 1988.

[22] J. M. J. Madey, "Stimulated Emission of Bremsstrahlung in a Periodic Magnetic Field", *Journal of Applied Physics* 42, 1906 (1971); https://doi.org/10.1063/1.1660466

[23] In Soo Ko, Heung-Sik Kang, Hoon Heo, Changbum Kim, Gyujin Kim, Chang-Ki Min, *et al.*, "Construction and Commissioning of PAL-XFEL Facility", *Appl. Sci.* 2017, 7(5), 479; https://doi.org/10.3390/app7050479

[24] S. Reiche, Genesis 1.3: a fully 3D time-dependent fel simulation code. Nuclear Instruments and Methods in Physics Research Section A: Accelerators, Spectrometers, Detectors and Associated Equipment, 429(1):243-248, 1999.